



Developing a deformable model of liver tumor during breathing to improve targeting accuracy in image-guided therapy using finite element simulation

Z. Matin Ghahfarokhi^a, M. Salmani-Tehrani^a, and M. Moghimi Zand^{b,*}

a. *Department of Mechanical Engineering, Isfahan University of Technology, Isfahan, P. O. Box 8415683111, Iran.*

b. *Small Medical Devices, Bio-MEMS & LoC Lab, School of Mechanical Engineering, College of Engineering, University of Tehran, Tehran, Postal Code 14399-55961, Iran.*

Received 3 October 2018; received in revised form 2 December 2018; accepted 12 January 2019

KEYWORDS

Breathing;
Finite element model;
Liver tissue;
Point cloud;
Tumor.

Abstract. Numerical simulation of the motion and deformation of a tumor embedded into the liver during respiration can help locate a tumor for radiotherapy. Here, a 3D Finite Element (FE) model is presented to simulate the behavior of the human liver during respiration. First, the point cloud data according to Computed Tomography (CT) image data was imported into CATIA software. Then, a spherical tumor was embedded into different segments of liver tissue in ABAQUS. A quasi-linear hyper-viscoelastic constitutive model and elastic behavior were considered to define the liver and tumor properties, respectively. Boundary conditions were defined based on the difference between end-exhale and end-inhale states of liver tissue. The deformation and motion of the liver tumor were then determined in the intermediate states of breathing. Finally, the new position and the deformed shape of the tumor were investigated, considering the increase of tumor stiffness. The results showed that the tumor located in the segment VII experienced maximum displacement in the y -direction. Similarly, maximum z -displacement was observed for the tumor embedded into segment VI, while the tumor embedded into segments II and V experienced maximum displacement in the x -direction. Moreover, the maximum motion took place for the tumor in segment VI.

© 2020 Sharif University of Technology. All rights reserved.

1. Introduction

After skin, liver is the second largest gland in the living body. It is the only organ that is able to regenerate, or renovate, itself by producing new cells. The liver performs many vital functions such as storing iron,

drug metabolism, maintaining the hormonal balance, and producing bile to help with food digestion [1–3]. On the other hand, liver cancer and chronic liver disease are the leading causes of death for more than 15000 Americans annually [3]. These important features and high mortality rates are convincing enough to include the liver in many biomechanical studies.

Nowadays, the use of computer-aided surgery technology is a significant progress in surgical planning for treating the diseases [4]. Computer-aided surgery, known as a minimally invasive method, results in small operative trauma in the human body, less pain,

*. *Corresponding author. Tel.: +98 021 61114807; Fax: +98 21 88013029 E-mail addresses: z.matin@alumni.iut.ac.ir (Z. Matin Ghahfarokhi); tehrani@cc.iut.ac.ir (M. Salmani-Tehrani); mahdimoghimi@ut.ac.ir (M. Moghimi Zand)*

less blood, shorter hospitalization time, and lower cost [5,6]. Nevertheless, a surgeon may experience some difficulty without a direct vision of the organs. Medical image methods, e.g., Computed Tomography scan (CT scan), Magnetic Resonance Image (MRI), and so on, play a major role in this technology [7]. However, the accuracy of image-guided therapy is considerably affected by tissue motion and deformation.

The breathing process is an important factor in the movement of tissues. During breathing excursions, the volume of the chest cavity increases, and the positions of organs close to the diaphragm are more affected than structures around the lung apices [8]. Hence, the liver deformation by breathing is a crucial factor, since liver is in connection with diaphragm [9]. Therefore, to precisely locate the tumor within the liver during interventional procedures is a challenging research subject [10]. To overcome this problem, several techniques have been used such as breath holding or taking into account a safety margin around the tumor [11]. In such cases, most of the patients who endure liver diseases are old and weak and, therefore, cannot cooperate well with the physician [12]. Therefore, considerable studies have been conducted to help physicians improve the treatment accuracy. Among these, Finite Element (FE) simulation is one of the most favorite methods that has been extensively used [13].

Nutu et al. [14] proposed and described a methodology to obtain the Finite Element Method (FEM) of the lung. The proposed method is based on the boundary condition of the lung’s outer surface. Therefore, through the application of the method, the displacement of different points within the organ during the breathing process can be predicted. Zehtabial et al. [15] studied the feasibility of creating a fast 3D model for simulating respiratory lung deformation. A similar study was also performed to provide infor-

mation on the lung-tumor motions due to breathing. The interested readers can refer to [16] for more information. Moreover, Lorente et al. [7] modeled the biomechanical response of the liver tissue in real time using the machine learning technique.

Only few studies have reported FE modeling and simulation of organs for facilitating targeting. Reviewing these studies reveals that none of them was focused on studying deformation and displacement of tumor within the liver. In this paper, a 3D FE model is developed to simulate the behavior of the human liver as a whole using CT image data. The main goal of this study is to investigate the motion and deformation of a tumor embedded into the liver during respiration. The results of this study are important for guiding surgeons during interventional procedures, when the liver tumor is to be located for radiotherapy treatment.

For this purpose, four different segments II, V, VI, and VII of the liver tissue were separately considered and studied as the tumor locations (Figure 1). The reason for choosing these segments is that segments II and VII are located under the diaphragm. Then, these segments endure much displacement. Then, the tumor motion in segments II and VII can be more than other segments. On the other hand, segments V and VI are located on the gallbladder and intestines, respectively. Moreover, the boundaries of segment V are adjacent to other parts, and we guess this proximity will cause less tumor shape in this segment. However, it is expected that the tumor located in segment VI will take more shapes because this segment is compressed by the upper parts of the intestines.

In Section 2, the biomechanical modeling and FE simulation of the human liver are described in detail. The results of simulations are illustrated in Section 3. In Sections 4 and 5, the simulation results and concluding remarks are presented, respectively.

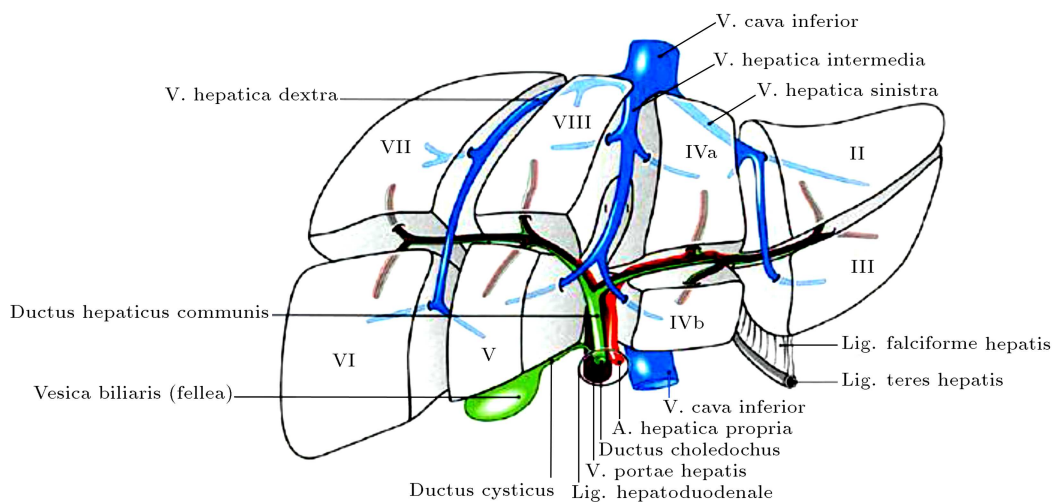


Figure 1. Segmental anatomy of the liver [17].

2. Materials and methods

This section is divided into two subsections. First, the biomechanical modeling for predicting the mechanical behavior of a human liver tissue is introduced in Section 2.1. Next, the method used for the FE simulation of liver is described in Section 2.2.

2.1. Biomechanical modeling of a human liver tissue

In this paper, the quasi-linear hyper-viscoelastic model, previously proposed by Fung [18], was adopted to model the mechanical response of the human liver tissue. In this model, the hyperelastic part is described as the reduced polynomial form of the strain energy function [19]:

$$w = c_{10} \left(J^{-\frac{2}{3}} I_1 - 3 \right) + c_{20} \left(J^{-\frac{2}{3}} I_1 - 3 \right)^2 + \frac{K}{2} (J - 1)^2. \quad (1)$$

Furthermore, the time-dependent material parameters are used to describe the viscoelastic part of the tissue behavior. For this purpose, relaxation function, $g(t)$, is defined and introduced in Eq. (2) [19]:

$$g(t) = 1 - \sum_{k=1}^2 g_k \left(1 - e^{-\frac{t}{\tau_k}} \right). \quad (2)$$

In Eq. (1), c_{10} ($i=1,2$) stand for the elastic material parameters; I_1 and J denote the first invariant of right Cauchy-Green deformation tensor and the determinant of the deformation gradient tensor, respectively. Moreover, K is the bulk modulus that characterizes the compressibility of the soft tissue. The parameters τ_k and g_k in Eq. (2) indicate the times and relaxation coefficients, respectively.

2.2. Preparing modeling the geometry

In order to demonstrate the displacement of the tumor in the liver tissue during the breathing process, the whole FE model of a tumor embedded into the human liver was created. First, the liver geometry was obtained from the point cloud according to CT image

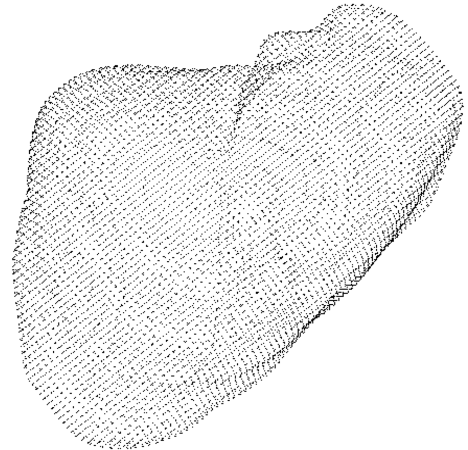


Figure 2. A point cloud of Computed Tomography (CT) image data for the normal human liver.

data, represented by Suwelack et al. [20], as shown in Figure 2.

By importing this point cloud into CATIA software, the curved surfaces have been constructed on the point cloud using the automatic surface option. Then, the closed surface option was used to convert the surface into a solid volume (Figure 3). The geometrical model was then imported into ABAQUS software. The mechanical properties were assigned to the FE model of the liver, as mentioned in Table 1.

The tumor was modeled as an elastic sphere of diameter 10 mm in the FE simulations. Table 2 presents the tumor location zone within the liver parenchyma. The values of 8 kPa and 0.49 were assigned to Young's modulus and Poisson's ratio of the tumor, respectively [21,22].

In the next step, the liver was meshed using 4-node linear tetrahedron, hybrid element (C3D4H), and the model of the tumor consists of 1242, the 8-node linear brick, hybrid elements. The mesh of the tumor within the liver is shown in Figure 4.

The boundary conditions were defined based on the difference in the position of the liver regions in the end-exhale and end-inhale states [23]. Both the displacement and deformation of the tumor with

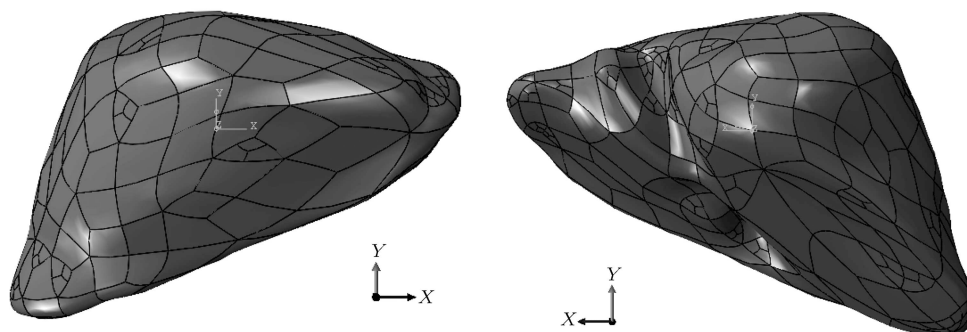


Figure 3. Geometry of the finite element model for the human liver.

Table 1. The material parameters of the liver [19].

c_{10} (kPa)	c_{20} (kPa)	g_1	τ_1 (s)	g_2	τ_2 (s)
9.85	26.29	0.51	0.58	0.15	6.89

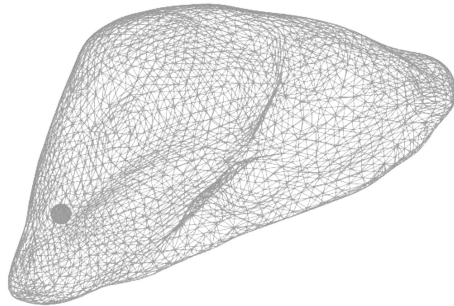


Figure 4. The meshed Finite Element (FE) model of the tumor within the human liver.

different stiffnesses were evaluated and determined to provide the data that can help improve the accuracy of image-guided procedures.

3. Results

Table 3 reports the position of the tumor at the end of the breathing period. The results show that the initial range of x , y , and z coordinates of the tumor within the left lobe is (71.127 to 81.127 mm), (20.3 to 30.3 mm), and (95 to 105 mm), respectively. These coordinate

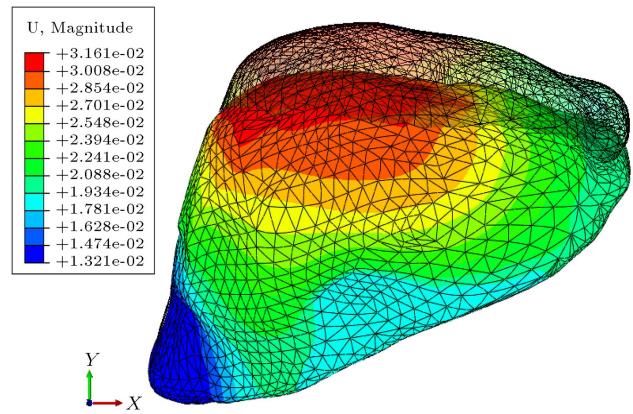


Figure 5. The displacement of the liver parenchyma in a breathing cycle.

ranges have changed to (67.8259 to 78.0354 mm), (3.41504 to 13.2503 mm), and (106.152 to 112.303 mm) at the end of the breathing period.

The effect of tumor stiffness is shown in Table 4. In this table, the location of the tumor in segment VI is investigated when the tumor stiffness increases by a factor of 6.25. This result suggests that the tumor moves by a value of 2.09 mm at Young’s modulus of 8 kPa.

Figure 5 plots the displacement of the liver parenchyma in a breathing cycle. As is seen, the upper surface of the liver endures higher displacement than other sections because of being placed under the diaphragm. Among segments II and VII, the

Table 2. The position of the tumor within the liver.

Model no.	Location in liver	X(mm)	Y (mm)	Z (mm)
1	Segment VII	−21.464 to −31.464	26.748 to 36.748	95 to 105
2	Segment VI	−69.816 to −79.816	−45.887 to −55.887	95 to 105
3	Segment II	71.127 to 81.127	20.3 to 30.3	95 to 105
4	Segment V	−25.802 to −35.802	−57.132 to −67.132	95 to 105

Table 3. The final position of the tumor within the liver.

Model no.	X (mm)	Y (mm)	Z (mm)
1	−29.4616 to −40.4237	4.9948 to 13.8333	109.281 to 119.865
2	−71.4393 to −81.0651	−61.0469 to −70.0071	100.578 to 112.36
3	67.8259 to 78.0354	3.41504 to 13.2503	106.152 to 112.303
4	−28.5048 to −38.1829	−75.892 to −86.61464	98.1535 to 108.203

Table 4. The position of the tumor in segment VI for different stiffness rates.

Young’s modulus (kPa)	X (mm)	Y (mm)	Z (mm)
8	−71.4393 to −81.0651	−61.0469 to −70.0071	100.578 to 112.36
10	−71.4165 to −81.0768	−61.0249 to −70.0274	100.567 to 112.363
20	−71.3475 to −81.1072	−60.9565 to −70.0895	100.541 to 112.362
50	−71.12724 to −81.1187	−60.8723 to −70.1571	100.548 to 112.307

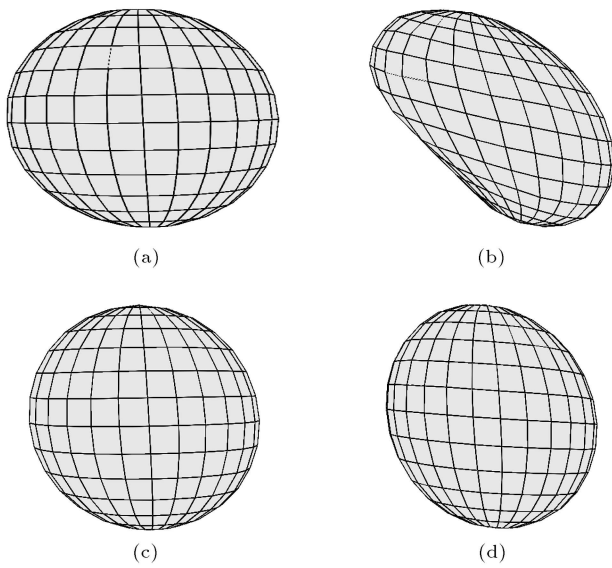


Figure 6. Displacement map of the deformed tumor in (a) segment VII, (b) segment VI, (c) segment II, and (d) segment V.

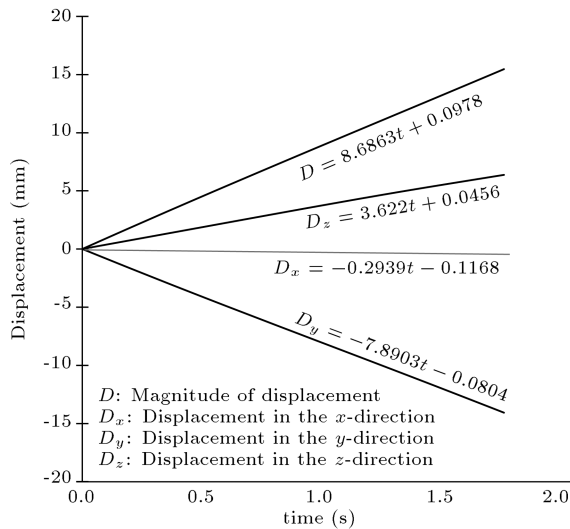


Figure 7. Displacement of the tumor during the breathing process.

former is highly constrained due to its contact with the stomach and is slower in motion. Moreover, segment VI experiences lower displacement rather than segment V due to its location on the intestines. However, the shape of the tumor in segment VI is large because of its compression between segment VII and the intestines. Moreover, Figure 6 represents the displacement map of the deformed tumor in different locations of the liver parenchyma. In order to assess the motion planning of the tumor, the displacement below the tumor point located in segment VI is displayed in Figure 7. Moreover, stress distribution through the liver tumor is illustrated in Figure 8. In addition, Figure 8 shows that stress is uniformly distributed.

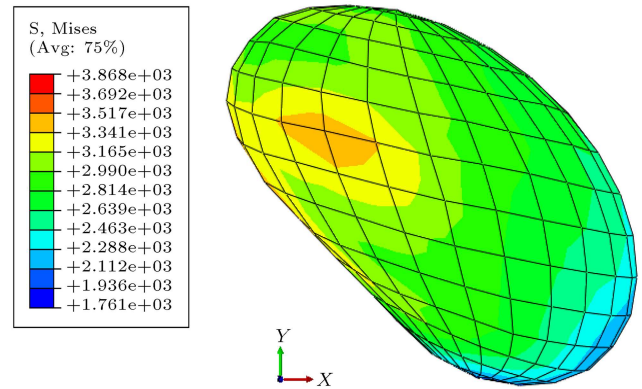


Figure 8. Stress distribution through the liver tumor.

4. Discussions

Computer-aided technology is recognized as a significant progress in treating liver diseases, especially for the image-guided therapy, in which tumor motion and deformation are required. The respiratory process is an important challenge in locating the tumor.

In this paper, a 3D model of the tumor within the human liver tissue was simulated using CT image data to assess the displacement of the tumor and its relation to breathing stages. The primary purpose is to demonstrate how the liver tumor moves and takes shape during the breathing process. The secondary purpose is to investigate how the shape of the tumor changes the increasing tumor stiffness.

The results of this study showed that for the tumor located in segment VII, maximum displacement was observed in the *y*-direction. However, maximum displacement for segment VI was recorded in the *z*-direction and, also, occurred for segments II and V in the *x*-direction. Moreover, the maximum shape value of the liver tumor was found in segment VI. Additionally, the tumor stiffness did not significantly affect the magnitude of motion and deformation. In the breathing stages, the tumor was displaced on a plan based on the first order.

The validity of the obtained results is difficult because of the lack of a similar research task. However, this method can be the basis of the 4D dynamic model development using intermediate positions of the tumor calculated from end-inhale to end-exhale. Knowing this information, a physician can better determine how tumor motion affects the required dose during radiation therapy and, thus, surgeons are able to demonstrate the tumor location.

5. Conclusions

In this work, the whole finite element model of the human liver tissue was simulated to target the tumor embedded into the liver during respiration. The tumor was located in different positions of the liver

parenchyma. This model provided a prediction of the tumor displacement map using only one Computed Tomography (CT) image data in the breathing stages. This investigation can potentially help surgeons improve the accuracy of targeting in the image-guided therapy of liver cancer patients.

Nomenclature

C_{i0}	Material parameter, kPa
I_1	First invariant of right Cauchy-Green deformation tensor
J	Determinant of the deformation gradient tensor
K	Bulk modulus
w	Strain energy function
g	Relaxation coefficient

Greek letters

τ	Relaxation coefficient, s
--------	---------------------------

References

1. Yarpuzlu, B., Ayyildiz, M., Enis Tok, O., et al. "Correlation between the mechanical and histological properties of liver tissue", *J. Mech. Beh. Biomed. Mat.*, **29**, pp. 403–416 (2014).
2. Matin Ghahfarokhi, Z., Moghimi Zand, M., and Salmani Tehrani, M. "Analytical solution and simulation of the liver tissue behavior under uniaxial compression test", *Modares Mech. Eng.*, **16**(9), pp. 47–56 (1395) (in Persian).
3. www.liverfoundation.org
4. Matin Ghahfarokhi, Z., Moghimi Zand, M., and Salmani Tehrani, M. "Proposing a new nonlinear hyperviscoelastic constitutive model to describe uniaxial compression behavior and dependence of stress-relaxation response on strain levels for isotropic tissue-equivalent material", *Sci. Iran.*, **26**(6), pp. 3202–3270 (2019).
5. Samur, E., Sedef, M., Basdogan, C., and et al. "A robotic indenter for minimally invasive measurement and characterization of soft tissue response", *Med. Image Anal.*, **11**, pp. 361–373 (2007).
6. Dehghani Ashkezari, H., Mirbagheri, A., Behzadipour, S., et al. "A mass-spring-damper model for real time simulation of the frictional grasping interactions between surgical tools and large organs", *Sci. Iran, B.*, **22**(5), pp. 1833–1841 (2015).
7. Lorente, D., Martínez-Martínez, F., Rupérez, M.J. et al. "A framework for modeling the biomechanical behavior of the human liver during breathing in real time using machine learning", *Expert Syst. Appl.*, **71**, pp. 342–357 (2017).
8. Baxa, J., Ferdova, E., and Ferda, J. "PET/MRI of the thorax, abdomen and retroperitoneum: Benefits of the breathing-synchronized scanning", *Eur. J. Radiol.*, **94**, pp. A35–A43 (2017).
9. Mescher, A.L., *Junqueira's Basic Histology*, McGraw Hill companies.
10. Dhont, J., Vandemeulebroucke, J., Burghelea, M., et al. "The long-and short-term variability of breathing induced tumor motion in lung and liver over the course of a radiotherapy treatment", *Radiother. Oncol.*, **126**(2), pp. 339–346 (2018).
11. Keall, P.J., Mageras, C.S., Balter, J.M., et al. "The management of respiratory motion in radiation oncology report of AAPM task group 76", *Med. Phys.*, **33**, pp. 3874–3900 (2006).
12. Srimathveeravalling, G., Leger, J., Ezell, P., et al. "A study of porcine liver motion during respiration for improving targeting in image-guided needle placements", *Int. J. CARS.*, **8**, pp. 15–27 (2013).
13. Saghaei Nooshabadi, Z., Abdi, E., Farahmand, F., et al. "A meshless method to simulate interactions between large soft tissue and a surgical grasper", *Sci Iran., B.*, **23**(1), pp. 295–300 (2016).
14. Nutu, E., Petrescu, H.A., Vlasceanu, D., et al. "Development of a finite element model for lung tumor displacements during breathing", *Mater. Today*, **3**, pp. 1091–1096 (2016).
15. Zehtabian, M., Faghihi, R., Mosleh-Shirazi, M.A., et al. "A fast model for prediction of respiratory lung motion for image-guided radiotherapy: A feasibility study", *Iran J. Radiat. Res.*, **10**(2), pp. 73–81 (2012).
16. Bäck, A. "Systematic evaluation of lung-tumor motion using four-dimensional computed tomography", *Phys. Med.*, **52**(1), pp. 3–4 (2018).
17. Paulsen, F. and Waschke, J., *Sobotta: Atlas der Anatomie des Menschen*, Urban & Fischer Verlag (2010).
18. Fung, Y.C., *Biomechanics, Mechanical Properties of Living Tissues*, Second Edn., Springer-Verlag, New York (1993).
19. Nava, A., Mazza, E., Furrer, M., et al. "In vivo mechanical characterization of human liver", *Med. Image Anal.*, **12**, pp. 203–216 (2008).
20. Suwelack, S., Roehl, S., Dillmann, R., et al. "Quadratic corotated finite elements for real-time soft tissue registration", In *MICCAI workshop: Comput. Biomech. Med.* (2011).
21. Gordic, S., Ayache, J.B., Kennedy, P., et al. "Value of tumor stiffness measured with MR elastography for assessment of response of hepatocellular carcinoma to locoregional therapy", *Abdom. Radiol.*, **42**(6), pp. 1685–1694 (2017).
22. Leroy, A., Payan, Y., Voirin, D., et al. "Finite element model of the liver for computer-assisted hepatic tumor ablation", *5th Int. Symp. on Computer Meth. Biomech. and Biomed. Eng.*, Roma (2001).

23. Brock, K.K., Hollister, S.J., Dawson, L.A., et al. “Technical note: Creating a four-dimensional of the liver using finite analysis”, *Med. Phys.*, **29**(7), pp. 1403–1405 (2002). <http://onlinelibrary.Wiley.Com/Doi/10.1118/1.1485055/full>

Biographies

Zahra Matin Ghahfarokhi received her BSc and MSc degrees in Mechanical Engineering of Biosystem from Shahrekord University, Iran in 2008 and 2011, respectively. Now she is a PhD Student in Mechanical Engineering at the Department of Mechanical Engineering, Isfahan University of Technology, Iran.

Mehdi Salmani-Tehrani completed his undergraduate studies, MSc, and PhD degrees, all at Isfahan

University of Technology, Iran. He is now an Assistant Professor at Isfahan University of Technology, where he has been a faculty member since 2011. His research interest mainly focuses on metal forming analysis and, recently, on biomechanics studies.

Mahdi Moghimi Zand is a Faculty Member in the School of Mechanical Engineering, College of Engineering, University of Tehran, and the Director of Small Medical Devices, Bio-MEMS & LoC Lab. Dr. Moghimi Zand’s research is multi-disciplinary and revolves around Vibrations, N/MEMS, computational mechanics, biomedical engineering, and nanotechnology. He has also conducted different studies at the University of California at Berkeley, Georgia Institute of Technology, Sharif University of Technology, Michigan State University, and the University of Tehran.